Synthesis and magnetic characterization of Ln(III) complexes with 4,4′-bipyridine and crotonato as bridging ligands

Juan Carlos Muñoz [a], Ana María Atria [a,*], Ricardo Baggio [b], María Teresa Garland [c], Octavio Peña [d], Cristian Orrego [a]

[a] *Facultad de Ciencias Químicas y Farmacéuticas and CIMAT, Universidad de Chile, Olivos 1007 Casilla 233, Santiago, Chile*
[b] *Departamento de Física, Comisión Nacional de Energía Atómica, Avda. Gral. Paz 1499, 1650 San Martín, Buenos Aires, Argentina*
[c] *Departamento de Física, Facultad de Ciencias Físicas y Matemáticas and CIMAT, Universidad de Chile, Avda. Blanco Encalada 2008, Casilla 487-3, Santiago, Chile*
[d] *L.C.S.I.M./UMR 6511 CNRS/Institut de Chimie de Rennes, Université de Rennes1, Rennes, France*

Abstract

The crystal structure and magnetic characterization of an isostructural series of general formula $\{[Ln(crot)_3(H_2O)(bpy)_{1/2}]_2\}_n$ (crot, crotonate ($C_4H_5O_2$); bpy, 4,4′-bipyridine ($C_{10}H_8N_2$); Ln, Nd, Gd, Ho, Er, Y) is presented. The ninefold Ln coordination polyhedra form dimeric entities that are connected throughout the bpy units into infinite polymeric chains. All (but the yttrium) reported compounds present a weak antiferromagnetic interaction connecting metal centres.

Keywords: Lanthanide complexes; Coordination polymers; Magnetic behaviour

1. Introduction

Homonuclear systems with ligands that serve as molecular bridges between metal centres have received considerable attention in recent years [1–3]. A point of interest in this systems is the possibility to introduce another organic ligand as bridge that allows to obtain grid structures and cluster, which are not only interesting structurally, but also for their potential application as ion exchange, catalysis, molecular absorption, optical, electronic and magnetic areas [4–10].

Recently, we have focussed attention on the efficiency of crotonic acid to couple two Ln(III) ions. In a previous work, we have described the synthesis, structural and magnetic characterization of the lanthanides complexes displaying crotonate bridges. During the course of our investigation, we have found that the incorporation of diimines during the synthesis procedure allows the crystallization, through their inclusion as a neutral ligand, counterion, or also as external crystallization agent [11,12].

We present herein the crystal structure and magnetic characterization of an isostructural series of general formula $\{[Ln(crot)_3(H_2O)(bpy)_{1/2}]_2\}_n$, where crot: crotonate ($C_4H_5O_2$); bpy: 4,4′-bipyridine ($C_{10}H_8N_2$); Ln: Nd (**1**), Gd (**2**), Ho (**3**), Er (**4**) and Y (**5**).

2. Experimental

2.1. Synthesis

The five complexes were prepared using the same general method: a solution of 4,4′-bipyridine (1 mmol) in methanol was added to an aqueous solution containing

* Corresponding author. Tel.: +56 2 678 2864; fax: +56 2 737 0567.
E-mail address: aatria@ciq.uchile.cl (A.M. Atria).

Ln_2O_3 (1 mmol) and crotonic acid (6 mmol). The resulting mixture was refluxed for 24 h, filtered while hot and then concentrated to 25 ml. The filtrate was left at room temperature. On standing, suitable crystals for single crystal X-ray diffraction appeared and were used without further processing.

2.2. Crystal structure determination

Highly redundant diffractometer data sets were collected at room temperature ($T = 295$ K) for all five structures up to a 2 (max. of ca. 58°) with a Bruker AXS SMART APEX CCD diffractometer using monochromatic Mo K radiation (=0.71069 Å) and a 0.3° separation between frames. For each one, data integration was performed using SAINT and a semi-empirical absorption correction was applied using SADABS, both programs being included in the diffractometer package. In all cases, the structure resolution was achieved routinely by direct methods and difference Fourier. The structures were refined by least squares on F^2 with anisotropic displacement parameters for non-H atoms.

In all five structures, hydrogen atoms attached to carbon (C–H's) were placed at their calculated positions and allowed to ride onto their host carbons both in coordinates as well as in thermal parameters. Terminal methyl groups were allowed to rotate as well. The aqua hydrogens were searched in the late Fourier maps, and freely refined with isotropic displacement factors.

All calculations to solve the structures, refine the proposed models and obtain derived results were carried out with the computer programs SHELXS 97 and SHELXL 97 [13], and SHELXTL/PC [14]. Full use of the CCDC package was also made for searching in the CSD Database [15].

Pertinent results are given in Tables 1–4, and Figs. 1–4, respectively.

2.3. Magnetic susceptibility measurements

Magnetic susceptibility data were collected on powdered samples, by using a SQUID magnetometer (QUANTUM Design Model MPMS–XL5 instrument) with a field of 0.1 T. The magnetic susceptibility data were corrected for the diamagnetism of the constituent atoms using Pascal's constants.

3. Results and discussion

3.1. Crystal structures

Table 1 presents a complete survey of crystallographic and refinement data for all five isostructural compounds. They crystallize in the triclinic space group $P\bar{1}$, and the asymmetric units (Fig. 1) are composed of a nine-coordinated Ln cation, three crotonato ligands, one aqua and one independent half of a whole bpy unit, bisected by a symmetry centre.

In the following we shall describe compound (**1**), the Nd moiety, as representative of the whole series, pointing out any significant difference with the rest, when pertinent.

The cation coordination sites are provided by six oxygens from three different crotonato units attached in a chelating mode, one of which acts also in a bridging mode linking to a near Ln neighbour and thus providing a seventh site. The independent bpy nitrogen and the aqua oxygen complete the ninefold sphere. The latter (Fig. 2) can be described as conformed by a pentagonal basal plane containing the cation and O7W, N1, carboxylate (O3, O4), and the bridging O5 $[1 - x, 2 - y, 2 - z]$, from a neighbouring unit. The plane is rather ill defined, with a mean deviation from the plane of 0.36 Å. The basal plane is in turn capped at both sides by two carboxylate groups, (O1,O2) and (O5,O6) which are almost orthogonal to the plane (91.4° and 92.3°, respectively) and very nearly so, to each other (99.6°).

Coordination distances span the range 2.430(2)–2.663(2) Å, and can be considered normal for this kind of complexes. As often happens, the carboxylato groups bite in a asymmetric way, with bond differences which range from 1.8% in (O3,O4) to 6.3% in (O5,O6). However, the most conspicuous difference is to be found in the two coordination modes of O5 (9.6%), the shortest (strongest) being the bridging one responsible for the dimeric loop.

Table 2 shows a comparison of coordination distances in all five complexes, presented in atomic number order. Distances show the same internal sequence and fall off from left to right, as expected for the well known lanthanide contraction, including the alien Yttrium at the end.

The $[Ln(crot)_3(H_2O)(bpy)_{1/2}]$ group already described acts as the elemental motive of a linear array, through the multiplicative effect of two independent symmetry centres in the structure. The one at (1/2,1,1) generates dimeric units by joining neighbouring coordination polyhedra through a $[Ln–O]_2$ loop, which in this case are characterized by a Ln…Ln distance of 4.231(1) Å and a Ln–O–Ln angle of 112.3(2)°.

The centre at (1,1,1/2), which duplicates the independent pyridyl group into a complete bpy molecule, acts as the linkage between dimeric units and making so a linear chain that runs parallel to $\langle -1\,0\,1\rangle$ which distinguishes the structure (Fig. 3). Each chain interacts with the neighbouring in a complex way making the whole structure a rather interesting coordination compound.

Non-bonding interactions are mainly of the H-bond type, with the two contacts involving the aqua hydrogens being by far the strongest. Table 3 (where only

Table 1
Crystal and refinement data for structures **1**, **2**, **3**, **4** and **5**

Compound, Ln	**1**, Nd	**2**, Gd	**3**, Ho	**4**, Er	**5**, Y
F_w	495.59	508.60	516.28	518.61	440.26
Crystal shape, colour	polyhedron, orange	polyhedron, yellow	polyhedron, colorless	polyhedron, red	polyhedron, colorless
a (Å)	8.3027(6)	8.2277(9)	8.201(2)	8.1873(5)	8.173(2)
b (Å)	10.5110(8)	10.4630(11)	10.450(3)	10.4403(7)	10.403(3)
c (Å)	11.9177(9)	11.8266(13)	11.788(3)	11.7809(8)	11.757(3)
α (°)	108.0050(10)	108.190(2)	108.228(3)	108.3010(10)	108.226(4)
β (°)	106.1360(10)	105.794(2)	105.639(3)	105.4640(10)	105.614(4)
γ (°)	97.3180(10)	97.364(2)	97.369(4)	97.4750(10)	97.420(4)
V (Å^3)	923.90(12)	905.06(17)	898.6(4)	895.95(10)	889.3(4)
d_{calc} (g cm^{-3})	1.781	1.866	1.908	1.922	1.644
$F(000)$	492	500	506	508	450
μ (mm^{-1})	2.848	3.703	4.441	4.723	3.319
θ Range	1.91–27.97	1.92–27.88	1.93–27.90	1.93–27.92	1.93–27.91
Index range	$-10 \leqslant h \leqslant 10, -13 \leqslant k \leqslant 13, -15 \leqslant l \leqslant 15$	$-10 \leqslant h \leqslant 10, -13 \leqslant k \leqslant 13, -15 \leqslant l \leqslant 15$	$-10 \leqslant h \leqslant 10, -13 \leqslant k \leqslant 13, -15 \leqslant l \leqslant 15$	$-10 \leqslant h \leqslant 10, -13 \leqslant k \leqslant 13, -15 \leqslant l \leqslant 15$	$-10 \leqslant h \leqslant 10, -13 \leqslant k \leqslant 13, -15 \leqslant l \leqslant 14$
Data, R_{int} parameters	3951(0.0145), 246	3892(0.0476), 246	3877(0.0166), 246	3811(0.0162), 246	3758(0.0560), 246
R_1,[a] wR_2[b] [$F^2 > 2\sigma(F^2)$]	0.0199, 0.0492	0.0457, 0.0821	0.0194, 0.0481	0.0197, 0.0467	0.0602, 0.1251
R_1,[a] wR_2[b] [all data]	0.0208, 0.0498	0.0610, 0.0870	0.0207, 0.0485	0.0207, 0.0472	0.1061, 0.1423
Maximum and minimum peaks (e Å^{-3})	0.634 and −0.382	0.919 and −0.996	0.944 and −0.633	0.712 and −0.854	1.041 and −0.808

Common items. General formula, $C_{17}H_{21}LnNO_7$; crystal system, triclinic; space group, $P\bar{1}$; Z, 2; temperature, 295 K.

[a] R_1: $\sum||F_o| - |F_c||/\sum|F_o|$.

[b] wR_2: $[\sum[w(F_o^2 - F_c^2)^2]/\sum[w(F_o^2)^2]]^{1/2}$.

Table 2
Selected bond lengths (Å) and angles (°) for **1**, **2**, **3**, **4** and **5**

Compound, Ln	**1**, Nd	**2**, Gd	**3**, Ho	**4**, Er	**5**, Y
Ln(1)–O(5)#1	2.430(2)	2.372(4)	2.340(2)	2.330(2)	2.324(4)
Ln(1)–O(2)	2.461(2)	2.398(4)	2.361(2)	2.347(2)	2.346(4)
Ln(1)–O(3)	2.469(2)	2.421(4)	2.382(2)	2.370(2)	2.376(4)
Ln(1)–O(7W)	2.479(2)	2.417(5)	2.378(2)	2.360(2)	2.363(5)
Ln(1)–O(6)	2.504(2)	2.437(4)	2.399(2)	2.386(2)	2.378(4)
Ln(1)–O(4)	2.513(2)	2.467(4)	2.444(2)	2.435(2)	2.431(4)
Ln(1)–O(1)	2.535(2)	2.495(4)	2.475(2)	2.468(2)	2.468(4)
Ln(1)–N(1)	2.661(2)	2.607(5)	2.567(2)	2.554(2)	2.566(4)
Ln(1)–O(5)	2.663(2)	2.636(4)	2.631(2)	2.633(2)	2.634(4)
Ln(1)...Ln(1′)	4.231(1)	4.174(2)	4.155(1)	4.152(1)	4.145(2)
Ln(1)–O(5)–Ln(1′)	112.3(1)	112.3(1)	113.3(1)	113.4(1)	113.3(1)

Symmetry code. $1' - x, 2 - y, 2 - z$.

Table 3
Hydrogen bonds for **1** (Å and °)

D–H...A	*d*(D–H)	*d*(H...A)	*d*(D...A)	∠(DHA)	Contact
C(4)–H(4C)...O(6)#2	0.96	2.48	3.409(4)	161.8	**
C(16)–H(16)...O(6)#3	0.93	2.42	3.345(3)	173.2	**
C(17)–H(17)...O(4)	0.93	2.40	3.091(3)	131.1	*
O(7W)–H(1W)...O(3)#1	0.85(4)	1.89(4)	2.727(3)	170(3)	*
O(7W)–H(2W)...O(1)#4	0.83(4)	1.87(4)	2.697(3)	176(3)	**

Symmetry codes. #1 $-x+1, -y+2, -z+2$; #2 $x,y-1, z$; #3 $-x+1, -y+2, -z+1$; #4 $-x+2, -y+2, -z+2$.
Contact type code. *, intrachain; **, interchain.

Table 4
Selected parameters describing the magnetic behaviour of **1**, **2**, **3** and **4**

Compound Ln	Temperature ranges (K)		θ (K)	C ($cm^3\ mol^{-1}\ K$)	μ_{eff} (MB)
	Measurement	Curie–Weiss			
(**1**) Nd	5–300	50–300	−39.48	3.31	3.42 (300 K) 2.30 (5 K)
(**2**) Gd	6–300	6–300	−0.22	14.22	7.52
(**3**) Ho	4–300	40–300	−8.22	26.59	10.14 (300 K) 7.42 (4 K)
(**4**) Er	5–300	50–300	−12.1	2.74	8.97 (300 K) 7.63 (5 K)

the interactions corresponding to structure (**1**) have been quoted, for simplicity) shows the effect quite clearly. Some of these interactions (marked as * in Table 3) enhance the intra-chain cohesion, while the remaining ones (**) provide to the inter-chain interaction. There is an extra, rather weak inter-chain π–π interaction linking double bonds of crotonato groups related by the symmetry centre at 0,1/2,1/2, where the corresponding C=C bonds, parallel to each other as required by symmetry, appear 3.69 Å apart and a slippage angle of less than 4°.

In spite of the rather bulky Ln coordination sphere, the specific cell volume per cation is quite low, spanning from 462 $Å^3$ (for Ln = Nd) down to 445 $Å^3$ (for Ln = Y). These low values are not only the lowest found for any Ln(crot) structure reported, but also fit in the lowest 15% percentile of all Ln complexes in the CSD, which points out to a very efficient packing of the Ln cations in the structures herein reported.

3.2. Magnetic results

The magnetic properties of the four lanthanide complexes in the series (Ln: Nd, Gd, Ho, Er) are summarized in Table 4, and their χ_m^{-1} and $\chi_m T$ behaviour (χ_m, molar susceptibility; T, temperature) represented as a function of T in Fig. 4.

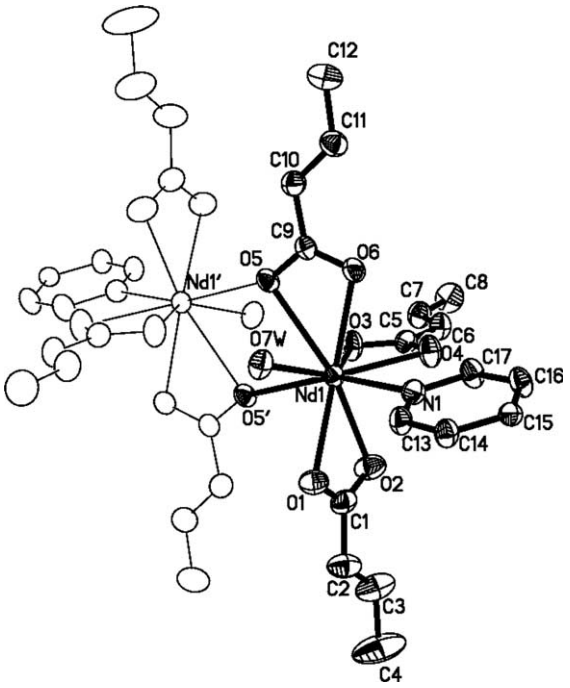

Fig. 1. Molecular diagram of **1** with displacement ellipsoids at 50% probability level, showing the numbering scheme used. Highlighted, the independent part of the structure plus O5′ which completes the metal coordination sphere. All hydrogen atoms removed, for clarity.

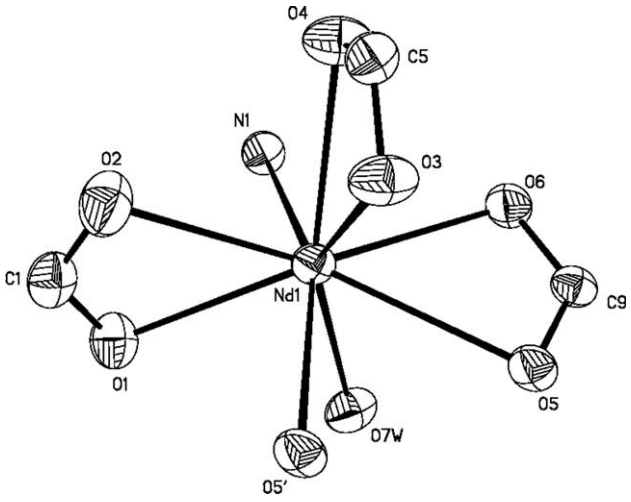

Fig. 2. Schematic diagram of the Ln coordination polyhedron in (**1**), displacement ellipsoids are shown at 50% probability level.

Values of θ and C were obtained from the least squares fit of those parts of the data sets, which appear to follow a Curie–Weiss law. The low negative value of θ (of variable magnitude) indicates for all compounds a (variably) weak antiferromagnetic interaction between metal centres. Inspection of Fig. 4 allows further consideration to be made, viz.:

Nd (**1**): $\chi_m T$ presents a monotonically decreasing behaviour with T, starting at 300 K with a maximum value $\chi_m T = 2.94\ \mathrm{cm^3\ mol^{-1}\ K}$, which implies a magnetic moment of 3.42 MB. This is the expected value for a magnetically isolated Nd(III) ion. At 5 K, the $\chi_m T$ value amounts to $1.33\ \mathrm{cm^3\ mol^{-1}\ K}$, giving a magnetic moment of 2.30 MB.

Gd (**2**): $\chi_m T$ is essentially constant along the whole temperature range. The mean value obtained ($\chi_m T \approx 14.15\ \mathrm{cm^{-3}\ mol^{-1}\ K}$) gives a magnetic moment of 7.52 MB; this is close to the expected value for two non-interacting Gd(III) ions (7.94 MB).

Ho (**3**): A Curie–Weiss behaviour was only observed above 40 K. In the high temperature end (300 K) $\chi_m T = 25.72\ \mathrm{cm^3\ mol^{-1}\ K}$ provides a magnetic moment of 10.14 MB per holmium atom, which is the expected value for an Ho(III) in the $^5I_8$ ground state. The product $\chi_m T$ is found to decrease with decreasing temperature, slowly at first and more steadily below 100 K, to reach a final value of $13.77\ \mathrm{cm^3\ mol^{-1}\ K}$ at 4 K, with a magnetic moment of 7.42 MB.

Er (**4**): The Curie–Weiss range was in this case 300–50 K. At 300 K, $\chi_m T = 20.12\ \mathrm{cm^3\ mol^{-1}\ K}$ led to a $\mu_{eff} = 8.97$ MB, in agreement with the expected value for two magnetically isolated Er(III) ions in the $^4I_{15/2}$ ground state. $\chi_m T$ decreases monotonically with temperature, with a final value $\chi_m T = 14.56\ \mathrm{cm^3\ mol^{-1}\ K}$ at $T = 5$ K. Such a behaviour is consistent with the thermal

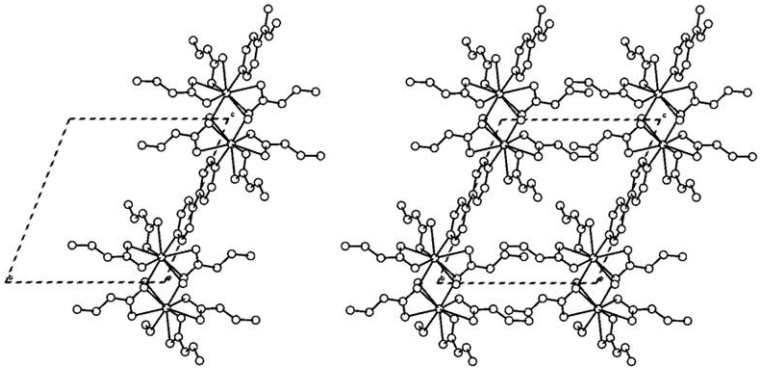

Fig. 3. Packing view of **1** projected down *a*-axis, showing one chain and the direction it runs throughout the unit cell and two parallel chains, showing a simplified packing pattern of the structure.

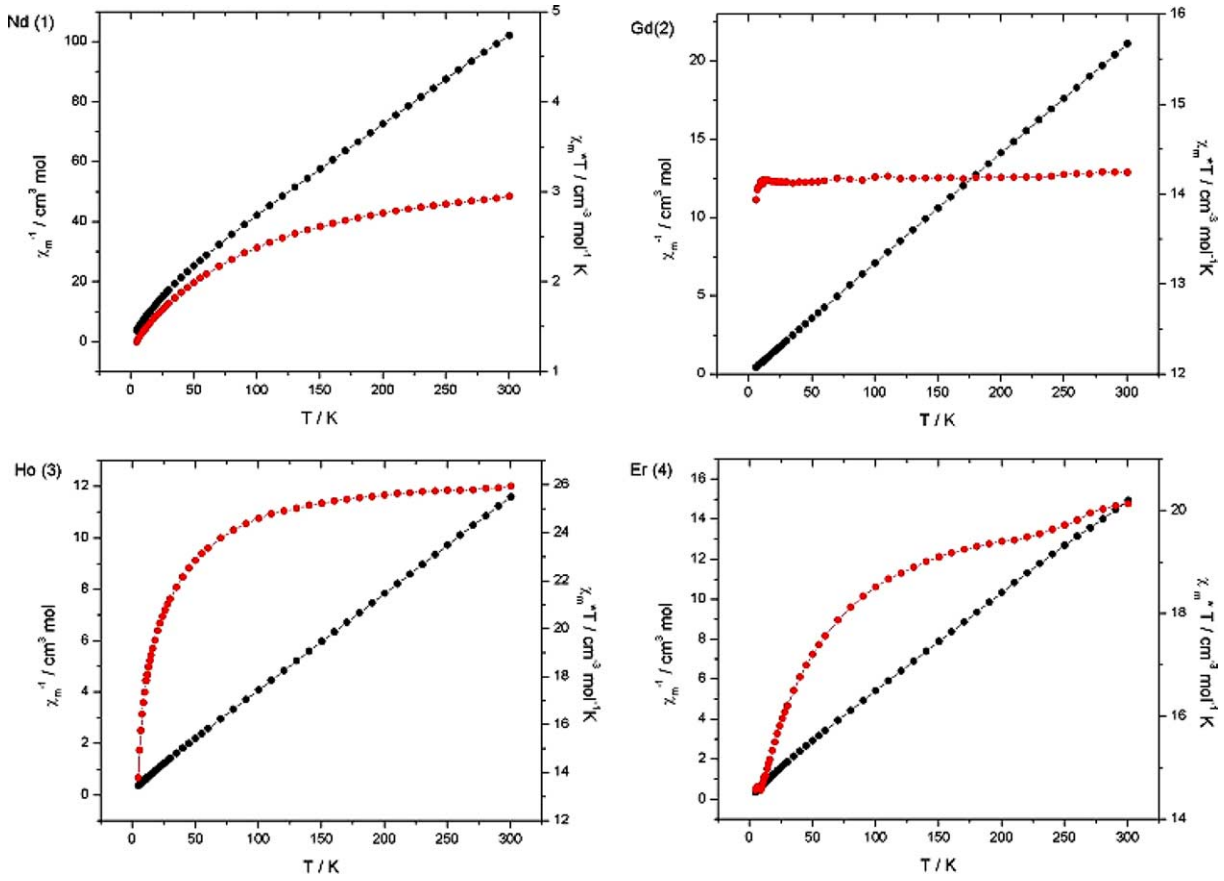

Fig. 4. Temperature dependence of χ_m^{-1} and $\chi_m T$ (χ_m: molar susceptibility) for **1**, **2**, **3** and **4**.

depopulation of the highest Stark components derived from the splitting of the free ion ground state.

In summary, we have isolated, characterized and reported structural data for four lanthanides crotonate complexes. The existence of these structures supports the feasibility of generating 2D and 3D polymeric complexes.

4. Supplementary material

Crystallographic data for the structural analysis have been deposited with the Cambridge Crystallographic Data Centre, CCDC Nos. 240324–240328 for (**1**)–(**5**), respectively. Copies of this information can be obtained free of charge from The Director, CCDC,12 Union Road, Cambridge, CB2 1EZ, UK (fax: +44 1223 336033, e-mail: linstead@ccdc.cam.ac.uk; or deposit@ccdc.cam.ac.uk).

Acknowledgements

The authors thank funding by FONDECYT (Project 1020802), FONDAP (Project 11980002), Fundación Andes (Project C-13575). O.P. acknowledges Region of Bretagne. J.C.M. is a grateful recipient of a Deutsdier Akademischer Austauschdient scholarship.

References

[1] L.K. Thompson, Coord. Chem. Rev. V. 233–234 (2002) 193.
[2] M. Fujita, J.W. Kwon, S. Washizu, J. Am. Chem. Soc. 116 (1994) 1151.
[3] J.Y. Lu, A.M. Babb, Inorg. Chem. Commun. 4 (2001) 716.
[4] R.-H. Wang, M.-C. Hong, W.-P. Su, Y.-C. Liang, R. Cao, Y.-J. Zhao, J.-B. Weng, Bull. Chem. Soc. Jpn. 75 (2002) 725.
[5] L. Pan, M.B. Sander, X. Huang, J. Li, M. Smith, E. Bittner, B. Bockrath, J.K. Johnson, J. Am. Chem. Soc. 126 (2004) 1308.
[6] D. Gatteschi, Adv. Mater. 6 (1994) 635.
[7] B.Q. Ma, D.S. Zhang, S. Gao, T.Z. Jin, C.H. Yan, Angew. Chem. Int. Ed. 39 (2000) 3644.
[8] D. Gatteschi, A. Caneschi, R. Sessoli, A. Cornia, Chem. Soc. Rev. 25 (1996) 101.
[9] G. Xu, Z.M. Wang, Z. He, Z. Lu, C.S. Liao, C.H. Yan, Inorg. Chem. 41 (2002) 6802.
[10] C. Benelli, D. Gatteschi, Chem. Rev. 102 (2002) 2369.
[11] A.M. Atria, C.J. Muñoz, A. Soto, M.T. Garland, R. Baggio, Acta Crystallogr., Sect. C 59 (2003) 416.
[12] A.M. Atria, R. Baggio, M.T. Garland, C.J. Muñoz, O. Peña, Inorg. Chim. Acta 357 (2004) 1997.

[13] G.M. Sheldrick, SHELXS-97 and SHELXL-97: Programs for Structure Resolution and Refinement, University of Göttingen, Germany, 1997.
[14] G.M. Sheldrick, SHELXTL-PC. Version 5.0, Siemens Analytical X-ray Instruments, Inc., Madison, WI, 1994.
[15] F.H. allen, O. Kennard, Chem. Des. Autom. News 8 (1993).